MODELIZATION AND SIMULATIONS OF THE ATMOSPHERIC DUST DYNAMIC

M.P. Velasco, D. Usero, S. Jiménez,
J.L. Vázquez-Poletti, L. Vázquez
mp.velasco@upm.es, umdavid@mat.ucm.es, s.jimenez@upm.es,
jlvazquez@fdi.ucm.es, lvazquez@fdi.ucm.es

V Reunión de Ciencias Planetarias y Exploración del Sistema Solar
CPESS5 - 8 Junio 2015

Introduction

Dust aerosols have a direct effect on both surface and atmospheric heating rates, which are also basic drivers of atmospheric dynamics.

Aerosols cause attenuation of the solar radiation traversing the atmosphere, modeled by the **Lambert-Beer-Bouguer law**, where the aerosol optical thickness is approximated by **Angstrom law**.

The measure of the amount of solar radiation at the Martian surface will be useful to gain some insight into the following issues:

1) UV irradiation levels at the bottom of the Martian atmosphere to use them as an habitability index.
2) Incoming shortwave radiation and solar heating at the surface.
3) Relative local index of dust in the atmosphere.

Attenuation of the radiation

The attenuation of solar radiation traversing the atmosphere is modeled by the Lambert-Beer-Bouguer law:

The Lambert-Beer-Bouguer law establishes that the direct solar irradiance $F(\lambda)$ at the Mars's surface at wavelength λ is given by

$$F(\lambda) = DF_0(\lambda)e^{-\tau(\lambda)m}, \quad (1)$$

where $F_0(\lambda)$ is the spectral irradiance at the top of the atmosphere, m is the absolute air mass, D is the correction factor for the earth-sun distance, and $\tau(\lambda)$ is the total optical thickness at wavelength λ.

Foundations of propagation of radiation in a medium

Relevance of the aerosol optical thickness

The total optical thickness is the sum of:

- the molecular scattering optical thickness $\tau_r(\lambda)$,
- the absorption optical thickness for atmospheric gases (O_2, O_3, H_2O, CO_2...) $\tau_g(\lambda)$,
- and the aerosol optical thickness $\tau_a(\lambda)$, obtained by solar spectral irradiance measurements through **Angstrom Law**:

$\tau_a(\lambda)$ can be approximated over a limited wavelength range:

$$\tau_a^{-1} = \frac{\lambda^\alpha}{\beta}, \tag{2}$$

- α is related to the size distribution of the scattering particles,
- β is the extinction coefficient for 1 μm wavelength, which depends on the concentration of aerosols in the atmosphere.

In the particular case of the Martian solar irradiance, simulations of its radiative transfer have been obtained in [2] for $\alpha = 1{,}2$ and $\beta = 0{,}3$, corresponding to an aerosol optical thickness $\tau_a = 0{,}6$:

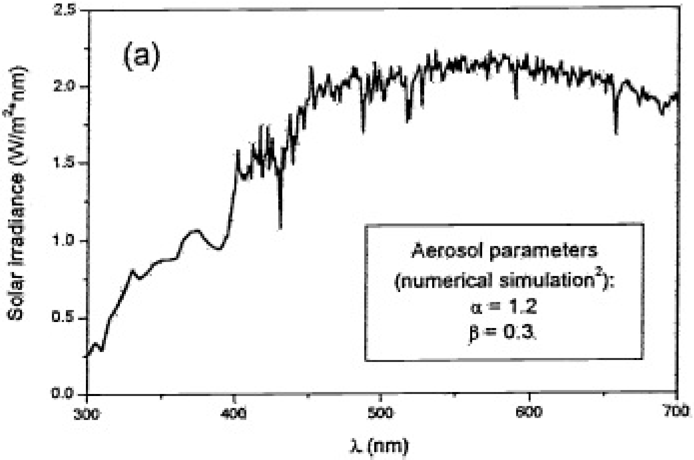

Fractional operators generalize ordinary derivatives and integrals from integer orders to non-integer orders.

The existence of different definitions of fractional operators allows a wide spectrum of possibilities to model real phenomena.

Caputo fractional derivative: Let $\alpha > 0$, $n-1 < \alpha < n$ and $n \in \mathbb{N}$, let D be the usual differential operator and let f be a suitable real function,

$$\frac{\partial^\alpha}{\partial t^\alpha} f(t) = \frac{1}{\Gamma(n-\alpha)} \int_0^x (t-s)^{n-\alpha-1} D^n f(s)\, ds \qquad t > 0, \alpha > 0. \tag{3}$$

$$\frac{\partial^\alpha}{\partial t^\alpha} E_\alpha(\lambda t^\alpha) = \lambda E_\alpha(\lambda t^\alpha), \qquad \alpha > 0, \lambda \in \mathbb{C}, \tag{4}$$

where $E_\alpha(z) = \sum_{k=0}^{\infty} \frac{z^k}{\Gamma(\alpha k + 1)}$ is known as **Mittag-Leffler function**.

A classical diffusion process is modeled by the diffusion equation

$$\frac{\partial \varphi}{\partial t} = c\frac{\partial^2 \varphi}{\partial x^2}, \tag{5}$$

then

- $\int_{-\infty}^{\infty} \varphi dx = 1$, and
- $\frac{d}{dt} < X^2 >= \int_{-\infty}^{\infty} x^2 \varphi_t dx = \int_{-\infty}^{\infty} x^2 c \varphi_{xx} dx = 2c$,

from which we obtain the classical mean square value, associated to the Brownian motion,

$$< X^2 >= \int_{-\infty}^{\infty} x^2 \varphi dx = 2ct. \tag{6}$$

Different modeling scenarios

Wavelength-fractional diffusion equation

Solar radiation in the atmosphere is governed by different time/space scales.

Thus, integro-differential equations could describe a better modelization.

$$\frac{\partial^\alpha \varphi}{\partial \lambda^\alpha} = \frac{\Gamma(\alpha+1)}{2\beta} \frac{\partial^2 \varphi}{\partial x^2}, \qquad 0 < \alpha < 2. \tag{7}$$

$$\begin{cases} \lim\limits_{x \to \pm\infty} \varphi(\lambda, x) = 0, & \lambda > 0 \\ \varphi(0+, x) = \delta(x), & x \in \mathbb{R}, \\ \frac{\partial}{\partial \lambda} \varphi(\lambda, x)\Big|_{\lambda=0} = 0 & (\text{condition for } 1 < \alpha < 2). \end{cases} \tag{8}$$

Solution or Green function is expressed through Mittag-Leffler or Wright function:

$$\varphi(\lambda, x) = \frac{1}{2\pi} \int_{-\infty}^{\infty} E_\alpha \left(-\frac{\Gamma(\alpha+1)}{2\beta} \lambda^\alpha \right) e^{-ikx} dk, \tag{9}$$

$$\varphi(\lambda, x) = \frac{1}{2\pi \lambda^{\alpha/2}} W \left(-\frac{|x|}{\lambda^{\alpha/2}} \left(\frac{\Gamma(\alpha+1)}{2\beta} \right)^{-1/2}; -\frac{\alpha}{2}; 1 - \frac{\alpha}{2} \right). \tag{10}$$

Different modeling scenarios

Second and higher order moments

$$< X^2 >= \int_{-\infty}^{\infty} x^2 \varphi(t,x) dx = \frac{1}{\beta}\lambda^{\alpha},$$

$$< X^{2n} >= \int_{-\infty}^{\infty} x^{2n} \varphi(\lambda,x) dx = \frac{\Gamma(2n+1)}{\Gamma(\alpha n+1)} \left(\frac{\Gamma(\alpha+1)}{2\beta}\lambda^{\alpha}\right)^n, \qquad n = 0,1,2...$$

Same $\tau_a(\lambda)$ under different conditions of diffusion or size of scattering particles

$$\frac{2c_1}{\Gamma(\alpha_1+1)}\lambda^{\alpha_1} = \frac{2c_2}{\Gamma(\alpha_2+1)}\lambda^{\alpha_2} \quad \Rightarrow \quad \lambda = \left(\frac{c_2\Gamma(\alpha_1+1)}{c_1\Gamma(\alpha_2+1)}\right)^{\frac{1}{\alpha_1-\alpha_2}}.$$

Relation between two aerosols, $\tau_{a,1}$ and $\tau_{a,2}$

- Relation between theirs aerosol optical thickness: $\frac{\tau_{a,2}}{\tau_{a,1}} = \frac{\beta_2}{\beta_1}\lambda^{\alpha_1-\alpha_2}.$
- Relation between theirs diffusion coefficients: $\frac{c_2}{c_1} = \frac{\Gamma(\alpha_2+1)\beta_2}{\Gamma(\alpha_1+1)\beta_1}.$

Different modeling scenarios

3D wavelength-fractional diffusion equation

$$\frac{\partial^\alpha \varphi}{\partial \lambda^\alpha} = \frac{\Gamma(\alpha+1)}{2\beta}\left(c_1\frac{\partial^2\varphi}{\partial x^2} + c_2\frac{\partial^2\varphi}{\partial y^2} + c_3\frac{\partial^2\varphi}{\partial z^2}\right), \qquad \alpha \in (0,1)\cup(1,2),$$

$$\begin{cases} \lim\limits_{\|\vec{x}\|\to\infty} \varphi(\lambda,\vec{x}) = 0, & \lambda > 0, \\ \varphi(0^+,\vec{x}) = g(\vec{x}), & \vec{x}\in\mathbb{R}^3, \\ \left.\dfrac{\partial}{\partial\lambda}\varphi(\lambda,\vec{x})\right|_{\lambda=0} = 0 & \text{(additional condition when } 1<\alpha<2), \end{cases}$$

where $\vec{x} = (x, y, z)$, and coefficients c_j, $j = 1, 2, 3$, taken as constants, correspond to possible anisotropies along the three spatial directions. The initial profile $g(\vec{x})$ may correspond, for instance, to the incoming solar irradiance reaching the top of the atmosphere.

3D wavelength-fractional diffusion equation: Radial symmetry case

Whenever the dust layers are stratified radially and the spatial dependence of φ is just with the distance and not the directions, we may consider the radial symmetry case. If the strata are homogeneous such that $c_1 = c_2 = c_3 = 1$, we perform a standard change of the function, defining $u(t,r) = r\varphi(t,r)$, and we have

$$\frac{\partial^\alpha u}{\partial \lambda^\alpha} = \frac{\Gamma(\alpha+1)}{2\beta}\frac{\partial^2 u}{\partial r^2}\,, \tag{11}$$

with

$$\begin{cases} \lim\limits_{r\to\infty} u(\lambda, r) = 0, & \lambda > 0, \\ u(0^+, r) = f(r), & r \in \mathbb{R}^+, \\ \dfrac{\partial}{\partial\lambda}u(\lambda, r)\Big|_{\lambda=0} = 0 & \text{(additional condition when } 1 < \alpha < 2), \end{cases} \tag{12}$$

Different modeling scenarios

3D wavelength-fractional diffusion equation: Radial symmetry case

Formally this is a 1D problem that we solve using the same techniques:

$$u(\lambda, r) = r\varphi(\lambda, r) = \frac{1}{2\pi}\int_{-\infty}^{\infty} E_\alpha\left(-\frac{\Gamma(\alpha+1)}{2\beta}k^2\lambda^\alpha\right)F(k)e^{-ikr}dk \quad (13)$$

$$= \sum_{j=0}^{\infty}\frac{f^{(2j)}(r)}{\Gamma(\alpha j+1)}\left(\frac{\Gamma(\alpha+1)}{2\beta}\lambda^\alpha\right)^j, \quad (14)$$

where F is the Fourier transform of f and $f^{(2j)}$ is the $2j$-order derivative of f.
If we consider $r \in [0, R]$ with fixed-end null boundary conditions, the solution is:

$$r\varphi(\lambda, r) = \sum_{k=1}^{\infty} c_k E_\alpha\left(-\frac{ck^2\pi^2}{R^2}\lambda\right)\sin\left(\frac{k\pi r}{R}\right), \quad (15)$$

where

$$c_k = \frac{2}{R}\int_0^R \sin\left(\frac{k\pi r}{R}\right) f(r)\,dr, \qquad E_\alpha(x) = \sum_{k=0}^{\infty}\frac{x^k}{\Gamma(\alpha k+1)}.$$

Numerical Methods

We define a discrete mesh with step size h for λ: $\lambda_n = nh$, and discrete meshes with a common step Δl for each of the spatial variables: $x_i = i\Delta l,\ y_j = j\Delta l,\ z_k = k\Delta l; i, j, k \in \mathbb{Z}$.

To represent the second order spatial derivatives we use standard, second order, centered, finite differences.

We have constructed two numerical methods for the 3D problem using two different approaches to the Caputo operator:

- the **Diethelm** representation, and
- the **Odibat** representation.

We use the notation:

$$\varphi_{n;\vec{\ell}} = \varphi(\lambda_n; x_i, y_j, z_k), \qquad \varphi_{n;i\pm1} = \varphi(\lambda_n; x_{i\pm1}, y_j, z_k),$$
$$\varphi_{n;j\pm1} = \varphi(\lambda_n; x_i, y_{j\pm1}, z_k), \qquad \varphi_{n;k\pm1} = \varphi(\lambda_n; x_i, y_j, z_{k\pm1}).$$

Numerical Methods

Diethelm Representation: Case $\mathbf{0} < \boldsymbol{\alpha} < \mathbf{1}$. *Truncation error:* $\mathcal{O}(\triangle\ell^2 h^{2-\alpha})$.

$$\frac{1}{h^{\alpha}\Gamma(2-\alpha)}\left(\varphi_{n;\vec{\ell}} - \varphi_{0;\vec{\ell}} + \sum_{m=1}^{n-1} d_{mn}\left(\varphi_{n-m;\vec{\ell}} - \varphi_{0;\vec{\ell}}\right)\right) = \frac{\Gamma(\alpha+1)}{2\beta}\cdot$$
$$\left(c_1\frac{\varphi_{n;i+1} - 2\varphi_{n;\vec{\ell}} + \varphi_{n;i-1}}{\triangle\ell^2} + c_2\frac{\varphi_{n;j+1} - 2\varphi_{n;\vec{\ell}} + \varphi_{n;j-1}}{\triangle\ell^2} + c_3\frac{\varphi_{n;k+1} - 2\varphi_{n;\vec{\ell}} + \varphi_{n;k-1}}{\triangle\ell^2}\right),$$

with: $d_{mn} = (m+1)^{1-\alpha} - 2m^{1-\alpha} + (m-1)^{1-\alpha}$, $0 < m < n$.

Diethelm Representation: Case $\mathbf{1} < \boldsymbol{\alpha} < \mathbf{2}$. *Truncation error:* $\mathcal{O}(\triangle\ell^2 h^{2-\alpha})$.

$$\frac{1}{h^{\alpha-1}\Gamma(3-\alpha)}\left(\theta_{n;\vec{\ell}} - \theta_{0;\vec{\ell}} + \sum_{m=1}^{n-1} e_{mn}\left(\theta_{n-m;\vec{\ell}} - \theta_{0;\vec{\ell}}\right)\right) = \frac{\Gamma(\alpha+1)}{2\beta}\cdot$$
$$\left(c_1\frac{\varphi_{n;i+1} - 2\varphi_{n;\vec{\ell}} + \varphi_{n;i-1}}{\triangle\ell^2} + c_2\frac{\varphi_{n;j+1} - 2\varphi_{n;\vec{\ell}} + \varphi_{n;j-1}}{\triangle\ell^2} + c_3\frac{\varphi_{n;k+1} - 2\varphi_{n;\vec{\ell}} + \varphi_{n;k-1}}{\triangle\ell^2}\right),$$

with: $\theta_{n;\vec{\ell}} = \frac{\varphi_{n+1;\vec{\ell}} - \varphi_{n-1;\vec{\ell}}}{2h}$, $e_{mn} = (m+1)^{2-\alpha} - 2m^{2-\alpha} + (m-1)^{2-\alpha}$, $0 < m < n$.

Odibat Representation: Case $\mathbf{0} < \alpha < \mathbf{1}$. *Truncation error:* $\mathcal{O}(\triangle\ell^2 h^2)$.

$$\frac{h^{-\alpha}}{\Gamma(3-\alpha)}\left[\varphi_{n+1,\vec{\ell}} - \varphi_{n-1,\vec{\ell}} + \sum_{m=1}^{n-1} C_{nm}\left(\varphi_{m+1,\vec{\ell}} - \varphi_{m-1,\vec{\ell}}\right)\right] = \frac{\Gamma(\alpha+1)}{2\beta}\cdot$$
$$\left(c_1\frac{\varphi_{n;i+1} - 2\varphi_{n;\vec{\ell}} + \varphi_{n;i-1}}{\triangle\ell^2} + c_2\frac{\varphi_{n;j+1} - 2\varphi_{n;\vec{\ell}} + \varphi_{n;j-1}}{\triangle\ell^2} + c_3\frac{\varphi_{n;k+1} - 2\varphi_{n;\vec{\ell}} + \varphi_{n;k-1}}{\triangle\ell^2}\right).$$

Odibat Representation: Case $\mathbf{1} < \alpha < \mathbf{2}$. *Truncation error:* $\mathcal{O}(\triangle\ell^2 h^2)$.

$$\frac{h^{-\alpha}}{\Gamma(4-\alpha)}\left[\varphi_{n+1,\vec{\ell}} - 2\varphi_{n,\vec{\ell}} + \varphi_{n-1,\vec{\ell}} + \sum_{m=1}^{n-1} C_{nm}\left(\varphi_{m+1,\vec{\ell}} - 2\varphi_{m,\vec{\ell}} + \varphi_{m-1,\vec{\ell}}\right)\right] = \frac{\Gamma(\alpha+1)}{2\beta}\cdot$$
$$\left(c_1\frac{\varphi_{n;i+1} - 2\varphi_{n;\vec{\ell}} + \varphi_{n;i-1}}{\triangle\ell^2} + c_2\frac{\varphi_{n;j+1} - 2\varphi_{n;\vec{\ell}} + \varphi_{n;j-1}}{\triangle\ell^2} + c_3\frac{\varphi_{n;k+1} - 2\varphi_{n;\vec{\ell}} + \varphi_{n;k-1}}{\triangle\ell^2}\right).$$

With $C_{nm} = (n-m+1)^{p-\alpha+1} - 2(n-m)^{p-\alpha+1} + (n-m-1)^{p-\alpha+1}, 0 < m < n$.
The computation of C_{nm} is much more costly than in the Diethelm approach.

We have implemented this numerical schemes.

The computational resources are demanding and we perform the ongoing simulations through **cloud computing**.

The final objective is to compare **numerical data** vs **real data**.

Do you have real data?
Can you lend us real data?
Please...

References

- V.E. Cachorro, A.M. de Frutos, J.L. Casanova, Determination of the Angstrom turbidity parameters, Applied Optics 26 (15), 3069-3076 (1987).
- C. Córdoba, L. Vázquez, Characterization of atmospheric aerosols by an in-situ photometric technique in planetary environments, in G.H. Bearman, P.M. Beauchamp (eds.), First Jet Propulsion Laboratory In Situ Instruments Workshop, SPIE, vol. 4878, 2003.
- A. Angstrom, On the atmospheric transmission of sun radiation and on dust in the air, Geografiska Annaler 11, 156-166 (1929).
- K. Diethelm, The analysis of fractional differential equations (Springer, New York, 2010).
- A.A. Kilbas, H.M. Srivastava, J.J. Trujillo, Theory and Applications of Fractional Differential Equations, Elsevier, Amsterdam, 2006.
- G.M. Zaslavsky, D. Baleanu, J.A. Tenreiro (Eds.), Fractional Differentiation and its Applications (Physica Scripta, 2009).
- M.P. Velasco, D. Usero, S. Jiménez, C. Aguirre, L. Vázquez, Mathematics and Mars Exploration, Pure and Applied Geophysics 172 (1), 33-47 (2015).

"The important thing is not to stop questioning" (Albert Einstein)

THANK YOU